NASA TECHNICAL MEMORANDUM

NASA TM X-3107

NASA TM X-3107

BOUNDARY-LAYER TRANSITION ON A PLATE SUBJECTED TO SIMULTANEOUS SPANWISE AND CHORDWISE PRESSURE GRADIENTS

by Donald R. Boldman and Paul F. Brinich

Lewis Research Center
Cleveland, Ohio 44135

NATIONAL AERONAUTICS AND SPACE ADMINISTRATION • WASHINGTON, D. C. • SEPTEMBER 1974

1. Report No.	2. Government Accession No.	3. Recipient's Catalog No.
NASA TM X-3107		

4. Title and Subtitle	5. Report Date
BOUNDARY-LAYER TRANSITION ON A PLATE SUBJECTED TO SIMULTANEOUS SPANWISE AND CHORDWISE PRESSURE GRADIENTS	SEPTEMBER 1974
	6. Performing Organization Code
7. Author(s)	8. Performing Organization Report No.
by Donald R. Boldman and Paul F. Brinich	E-7979
	10. Work Unit No.
9. Performing Organization Name and Address	501-24
Lewis Research Center National Aeronautics and Space Administration Cleveland, Ohio 44135	11. Contract or Grant No.
	13. Type of Report and Period Covered
12. Sponsoring Agency Name and Address	Technical Memorandum
National Aeronautics and Space Administration Washington, D. C. 20546	14. Sponsoring Agency Code

15. Supplementary Notes

16. Abstract

The boundary-layer transition on a short plate was studied by means of the china-clay visual technique. The plate model was mounted in a wind tunnel so that it was subjected to small simultaneous spanwise and chordwise pressure gradients. Results of the experimental study, which was performed at three subsonic velocities, indicated that the transition pattern was appreciably curved in the spanwise direction but quite smooth and well behaved. Reasonable comparisons between predictions of transition and experiment were obtained from two finite-difference two-dimensional boundary-layer calculation methods which incorporated transition models based on the concept of a transition intermittency factor.

17. Key Words (Suggested by Author(s))

Boundary layer
Boundary layer transition
Fluid mechanics
Transition

18. Distribution Statement

Unclassified - unlimited
Category 01

19. Security Classif. (of this report)	20. Security Classif. (of this page)	21. No. of Pages	22. Price*
Unclassified	Unclassified	31	$3.25

* For sale by the National Technical Information Service, Springfield, Virginia 22151

BOUNDARY-LAYER TRANSITION ON A PLATE SUBJECTED TO SIMULTANEOUS SPANWISE AND CHORDWISE PRESSURE GRADIENTS

by Donald R. Boldman and Paul F. Brinich

Lewis Research Center

SUMMARY

The boundary-layer transition on a short plate was studied by means of the china-clay visual technique. The plate model was mounted in a wind tunnel so that it was subjected to small simultaneous spanwise and chordwise pressure gradients. Results of the study, which was performed at three subsonic velocities, indicated that the transition pattern was appreciably curved in the spanwise direction but quite smooth and well behaved. Reasonable comparisons between predictions of transition and experiment were obtained from two finite-difference two-dimensional boundary-layer calculation methods which incorporated transition models based on the concept of a transition intermittency factor.

INTRODUCTION

Several years of research by numerous investigators have contributed to a reasonable understanding of the boundary-layer transition process for the simplest of flows, namely, the uniform flow along a smooth thin flat plate. In this classical case, transition predominately depends upon the Reynolds number and the turbulence intensity. However, in more complex flows, such as flows associated with blade rows in turbomachinery, other factors must be considered in analyzing the transition process. These include the pressure gradient (refs. 1 to 4) as well as the curvature, the surface roughness, the heat transfer, and three-dimensional effects (ref. 5).

The present experimental investigation was conducted in order to gain insight concerning the transitional behavior in a simple three-dimensional flow with no separation. The experiment described in this report represents an extension of the studies of simple uniform flow over a flat plate, since the plate model was subjected to small simultaneous spanwise and chordwise pressure gradients. Emphasis was placed on determining the ef-

fect of the resulting flow field on the transition patterns, with the streamwise pressure gradient and the free-stream turbulence intensity taken into account. The primary objectives of the study were (1) to determine whether the irregularities in transition pattern, often observed in two-dimensional boundary layers, would be present in a three-dimensional flow and (2) to ascertain how well the transition location could be predicted from contemporary two-dimensional boundary-layer calculations incorporating the experimental streamwise velocity distributions and turbulence intensity.

The experimental format for the present study was based in part on the transition study of reference 1, which treated the special cases of flow over rotating blades. In the present study, the three-dimensional flow was established by mounting the plate model between a curved lower wall and a flat upper wall of an otherwise two-dimensional flow channel. The china-clay visualization technique, which is described in reference 1, was used to determine the location of transition and to provide information on the regularity of transition in the spanwise direction.

Predictions of the transition location on rotating blades commonly employ the assumption of local two-dimensionality. This same assumption was applied in analyzing the boundary-layer development on the plate used in this study. Pressure measurements on the plate provided partial input to the boundary-layer theories of references 6 and 7, which incorporated different transition models. These transition models were based on a transition intermittency factor concept to describe the extent of the transition region. In this report experimental and predicted transitions are compared, and some of the practical aspects associated with the china-clay method of transition detection are discussed.

SYMBOLS

C_1	constant in eq. (3)
C_2	constant in eq. (4)
$\overline{K}$	pressure gradient parameter (eq. (10))
L	plate model length
P	stagnation pressure
p	static pressure
Re	Reynolds number
T	stagnation temperature
U	mean velocity in streamwise direction

u	fluctuating component of velocity in streamwise direction
u'	root-mean-square (rms) value of fluctuating component of velocity
X	nondimensional distance from plate model leading edge, x/L
x	distance from plate model leading edge
Y	distance from surface of upper wall of flow channel in normal direction
y	distance from surface of plate model in normal direction
Γ	transition intermittency factor ($0 \leq \Gamma \leq 1.0$)
γ	ratio of specific heats, 1.4
θ	boundary-layer momentum thickness
λ	transition length (eq. (9))
μ	viscosity
ν	kinematic viscosity
ξ	nondimensional distance from critical point (eq. (8))
ρ	density
ψ	streamline coordinate (eq. (1))

Subscripts:

cr	critical point where laminar instabilities begin
e	boundary-layer edge
eff	effective
LR	leading edge of plate model in plane of lower row of pressure taps (fig. 2)
LW	lower wall of wind tunnel in plane of plate model leading edge
P	potential flow
r	reference condition at upstream end of wind tunnel
t	transition
UR	leading edge of plate model in plane of upper row of pressure taps (fig. 2)
θ	based on momentum thickness
τ	turbulent flow
0	plenum
∞	free stream

APPARATUS AND INSTRUMENTATION

Facility

The present experiment was conducted in a 10.2- by 17.8-centimeter (4- by 7-in.) wind tunnel, which is described in reference 8. This tunnel, shown in figure 1, was operated with an atmospheric air inlet at a nominal plenum temperature of 22.2° C (72° F). Flow velocity was controlled by means of valves located downstream of the diffuser. An enlarged view of the test section showing the location of the plate model is also shown in figure 1. The test section portion of the channel consisted of a flat upper wall, curved lower wall, and flat glass side walls. The width of the upper and lower walls was 10.2 centimeters (4.0 in.), and the radius of curvature of the lower wall was 12.7 centimeters (5.0 in.). The leading edge of the plate model was located at the minimum cross-section area or throat of the tunnel, which had a height of 12.7 centimeters (5.0 in.). Preparation of the model prior to testing was facilitated by removing one of the glass side walls.

Plate Model

The plate model, which is shown in figure 2, had a chord length of 7.62 centimeters (3.0 in.) and span of 11.43 centimeters (4.5 in.). The plate was machined from brass and had a tapered forward section with a radius of curvature of 33.8 centimeters (13.3 in.). The leading edge tip radius was 0.025 centimeter (0.01 in.). The plate was instrumented with 14 static-pressure taps having inside diameters of 0.069 centimeter (0.027 in.). These taps were arranged in two rows and spaced as shown in figure 2. Pressures on the plate and in the wind tunnel were measured with tetrabromoethylene manometers referenced to the plenum pressure (nominally 1 atm).

FLOW CONDITIONS

Tests were conducted at nominal values of upstream reference velocity U_r ranging from 58 to 149 meters per second (190 to 489 ft/sec). The unit Reynolds number ranged from 3.61×10^6 to 8.53×10^6 per meter (1.1×10^6 to 2.6×10^6 per ft). The reference velocities were measured 25.4 centimeters (10 in.) upstream of the plate leading edge, where flow acceleration effects were negligible. The free-stream velocities near the lower leading edge pressure tap on the plate (fig. 2) were estimated to be from 80 to 241 meters per second (263 to 789 ft/sec).

RESULTS

Flow Field With No Model

Potential flow. - In order to gain some insight about the type of gradients encountered, a calculation was made of the potential flow field in the channel. It is recognized that the insertion of the plate model would alter this distribution to some extent. The results of the calculation, which were obtained from the program of reference 9, are shown in figure 3 for a reference velocity U_r of 91 meters per second (300 ft/sec). Maximum potential flow velocities at the upper and lower walls are 120 and 166 meters per second (394 and 544 ft/sec). The concentration of lines of constant static pressure on the lower wall indicates rapid axial changes in velocity on the lower wall relative to the upper wall. Also examination of the lines of constant pressure in the throat region reveals that the maximum velocity gradient across the channel occurs near the lower wall. The results from this potential flow calculation were used to estimate the free-stream velocity distribution at the leading edge of the plate model.

Boundary-layer velocity and turbulence intensity. - Results of hot-wire measurements of the velocity and turbulence intensity at four stations along the upper wall of the wind tunnel are presented in figures 4 and 5, respectively. These measurements were obtained at a reference velocity U_r of 94.4 meters per second (309.7 ft/sec). The profiles are plotted in terms of the streamline coordinate ψ/μ_0 and the dimensional coordinate Y. In the streamline coordinate system ψ/μ_0 represents the integrated mass flux from the wall to a distance Y from the wall, that is,

$$\frac{\psi}{\mu_0} = \frac{1}{\mu_0}\int_0^y \rho(Y)U(Y)\,dY \tag{1}$$

The values of velocity ratio and turbulence intensity at a given value of integrated mass flux (constant ψ/μ_0) lie along the same streamline. The velocity profiles in figure 4 are similar to those reported and discussed rather extensively in reference 8. The accelerated boundary layer of reference 8 had the usual "law of the wall" and "wake" regions for a turbulent boundary layer and, in addition, contained an outer inviscid rotational flow between the free-stream and conventional wake regions. This outer rotational region made it difficult to define an edge condition or thickness of the viscous boundary layer. As shown in figure 4(b), the boundary-layer thickness 2.5 centimeters (1.0 in.) downstream of the plate leading edge position was about 2.5 centimeters (1.0 in.) based on the distance from the wall in which the local velocity U attained the free-stream value U_∞. The corresponding thickness of the boundary layer on the lower

wall was less than the value for the upper wall (ref. 8).

The turbulence intensity profiles at the four stations on the upper wall are shown in figure 5. The turbulence intensity u'/U_∞ is the ratio of the rms value of the fluctuating component of velocity u to the local free-stream velocity U_∞, that is $u'/U_\infty \equiv \left(\overline{u^2}\right)^{1/2}/U_\infty$. The free-stream level of turbulence was determined from the minimum values of the distributions which occur at $\psi/\mu_0 = 1.5\times10^5$ (fig. 5(a)) or at a distance Y of about 2.5 centimeters (1.0 in.) (fig. 5(b)). The minimum values of u'/U_∞ ranged from about 0.018 at the upstream station to 0.033 at the station downstream of the plate leading edge position. The turbulence intensity in the plane of the plate leading edge was estimated from figure 5 to be no higher then 4 percent. This value should represent an upper limit since it was obtained with the plate model removed. The acceleration of the flow resulting from insertion of the plate model should attenuate the values of local free-stream turbulence intensity over the plate. Estimates of the turbulence intensity attenuation based on Batchelor's incompressible relations (ref. 10) indicated that the maximum attenuation for the flow conditions of this study would be only about 0.5 percent.

Experimental Transition on Plate Model

Model preparation. - The china-clay method of detecting transition is based on the principle that the rate of evaporation of a liquid film on the surface of a body is related to the local shear stress of the flow across the film. The preparation procedure which was followed in the present study was similar to that of reference 1. The brass plate model of this study was first blackened by spraying india ink on the surface. After the ink dried, a thin coating of china-clay solution was sprayed on the surface with an air-brush. This solution consisted of a mixture of about three parts of china clay to one part of airplane dope by volume thinned to spraying consistency with lacquer thinner. Upon drying, the plate model attained a uniform white appearance, as shown in figure 6. Prior to initiation of a test, the plate was sprayed with oil of wintergreen (methyl salicylate), which made the clay surface transparent and gave the plate the appearance of being black. During the test, the black oil-coated model became white as the oil evaporated. In regions of abrupt changes in shear stress, for example, transition, a well defined boundary could be determined from the contrast in appearance between the wet and dry portions of the model.

Experience indicated that the finish of the china-clay coating was an important factor in the transition process. For instance, if the plate was tested with small protuberances (caused by small lumps of china clay) on the surface, these roughness elements caused the boundary layer to become locally turbulent. The spreading of the turbulent flow downstream of the roughness elements could easily eradicate the natural transition re-

gion which otherwise would have been present on the plate. An illustration of the effect of these roughness elements is shown in figure 7. The photograph resolution is sufficient to detect some of the surface particles of clay which tripped the boundary layer and produced premature transition. The removal of these particles, particularly near the leading edge of the plate, was extremely important. The most satisfactory method of eliminating the effects of these random particles on the surface consisted of lightly buffing the china-clay surface coating with a soft cloth until a semigloss finish was attained.

The china-clay finish was sufficiently durable to permit several tests without the necessity of recoating the plate with clay. The duration of the tests was primarily a function of the mean flow velocity. At a reference velocity of 58 meters per second (190 ft/sec) drying times for the oil of wintergreen were from 3 to 4 minutes, whereas at the high reference velocity of 149 meters per second (489 ft/sec) the drying time was slightly less than 1 minute.

Interpretation of photographic data. - A sketch of a typical transition pattern on the plate is presented in figure 8. The dark region on the plate depicts the development of the laminar boundary layer. The white streak dividing the laminar boundary layer at the bottom row of pressure taps emanated from the turbulence generated by the leading edge pressure tap. A similar streaking occurred along the upper row of pressure taps; however, it is not as apparent because the diverging streak merges with the turbulent boundary layer associated with the tunnel wall. The transition line is the curved boundary between the dark wet region and the white dry region, which is near the center of the plate in the sketch of figure 8. The photographs (fig. 9) show that this boundary is fairly distinct and therefore should provide reasonable estimates of the transition location. It is difficult to assess the error in transition location without a more detailed knowledge of the boundary layer; however, based on the results of reference 1, the transition location determined from the china-clay method is probably within 5 percent downstream of the true position.

Transition photographs. - Transition photographs corresponding to reference velocities of 58, 87, and 149 meters per second (190, 285, and 489 ft/sec) are presented in figures 9(a) to (c), respectively. The dashed lines in the photographs represent the authors' interpretation of the transition location. The corresponding values of the nondimensional transition location X_t ($X = x/L$) are listed in table I.

The natural tendency for the transition line to move upstream with increasing velocity is apparent. This axial shift in the pattern is due primarily to the change in Reynolds number, that is, $x_t \alpha (\rho_\infty U_\infty)^{-1}$. The curvature in the transition patterns indicates that transition at the lower station always occurred upstream of the transition point at the upper station. This trend is consistent with the relative levels of local streamwise velocities, which were higher at the lower station (refer to fig. 3). However, it is difficult to

determine the extent to which the difference in the relative transition location on the plate might be attributed to the streamwise pressure gradient and free-stream turbulence intensity, exclusive of all other effects.

Transition Prediction Methods

The two-dimensional boundary-layer calculation methods of references 6 and 7 were used to obtain estimates of the transition location on the plate. The transition results from figures 9(a) and (c) were used in comparisons of experiment and theory, since these data represented extremes for the flow conditions considered. It was not the intent of this study to perturb the numerous input options associated with each method in order to obtain optimum agreement with the observed transition location. Instead, a recommended set of options was selected for each method, and the value of a single fundamental parameter in each method was varied in order to determine the effect on the predicted transition location. In the method of reference 6 this parameter was the critical vorticity Reynolds number Re_{cr}, whereas in the method of reference 7 the critical parameter was chosen to be the free-stream turbulence intensity u'/U_∞.

In reference 6 the differential forms of the equations of motion are solved in conjunction with an eddy viscosity modeling of the turbulence transport. The equations were solved by a three-point finite-difference method coupled with a fully implicit solution procedure. The eddy viscosity model consisted of a Van Driest inner region law and a Clauser outer region law (refer to ref. 6 for complete details).

The method of reference 7 utilizes the finite-difference implicit procedure of reference 11 to reduce the partial differential equations of motion to ordinary differential equations. The ordinary differential equations are then solved by a Gaussian elimination procedure. A three-layer model is used to describe the effective eddy viscosity (laminar plus turbulent viscosity). The reader should consult reference 11 for details.

Velocity distributions for boundary-layer calculations. - In applying the boundary-layer methods just discussed, it was necessary to specify a boundary-layer edge velocity distribution over the plate model. The edge velocity distributions were calculated from the measured wall static pressures by using the compressible flow relations for an isentropic perfect gas, that is,

$$U_e = \left\{ \frac{2\gamma RT_0}{\gamma - 1} \left[1 - \left(\frac{p}{P_0} \right)^{(\gamma-1)/\gamma} \right] \right\}^{0.5} \tag{2}$$

An exception was made to this procedure for determining the velocities at the leading edge pressure taps, which sensed a pressure close to the stagnation value. The

boundary-layer calculations were performed by assuming ideal flat plate leading edge conditions. An interpolation procedure was used to estimate the velocities at the leading edge stations. These estimated velocities were obtained from the values of measured velocity based on the lower wall pressure measurement relative to the potential flow at the lower wall and leading edge location (refer to fig. 3). This procedure had the advantage over linear interpolation between free-stream velocities at the upper and lower walls because it reflected the increasing rate of change of velocity in going from the upper flat wall to the lower curved wall. The interpolation method was based on simple ratios of the real and potential flow velocities given by

$$U_{\infty, LR} = C_1 U_{\infty, LW} \tag{3a}$$

where

$$C_1 = \left(\frac{U_{LR}}{U_{LW}}\right)_P \tag{3b}$$

and

$$U_{\infty, UR} = C_2 U_{\infty, LW} \tag{4a}$$

in which

$$C_2 = \left(\frac{U_{UR}}{U_{LW}}\right)_P \tag{4b}$$

The subscripts UR and LR denote the positions of the upper and lower leading edge pressure taps, respectively. The subscript LW denotes conditions associated with the lower curved wall of the wind tunnel in the plane of the plate leading edge, and the subscript P refers to the potential flow conditions given in figure 3. The constants C_1 and C_2 in equations (3) and (4) had values of 0.813 and 0.739, respectively. Additional potential flow calculations indicated that these values were within about 3 percent of the values for the other flow conditions of this study.

The experimental values of U_e are presented in table II and are plotted in figure 10 for the three test conditions given in figure 9. Additional values of U_e, used in the boundary-layer calculations, were obtained from a smoothed fairing of the data in table II.

Transition models. - The transition models incorporated in the boundary-layer calculation methods of references 6 and 7 were based on the concept of a transition intermittency factor Γ which attains values of $0 \leq \Gamma \leq 1.0$. This intermittency factor was

used to modify the effective viscosity in the transition region according to the following expression:

$$\nu_{eff} = \nu + \Gamma\nu_{\tau} \tag{5}$$

In the program of reference 6, the critical point or initial instability is prescribed in terms of a critical vorticity Reynolds number Re_{cr}, given by

$$Re_{cr} = \left[\left(\frac{y^2}{\nu}\frac{\partial U}{\partial y}\right)\right]_{cr} \tag{6}$$

The values of Re_{cr} are usually in the range 2000 to 4000 (ref. 6). The transition process was initiated when the specified value of Re_{cr} was reached. The expression for the intermittency factor in the transition region was obtained from reference 12, which shows that

$$\Gamma = 1 - \exp(-0.412\ \xi^2) \tag{7}$$

The value of ξ in equation (7) represents the ratio of the distance from the critical point to a transition length λ, which can be expressed as

$$\xi = \frac{x - x_{cr}}{\lambda} \tag{8}$$

The value of λ is a measure of the transition length, as discussed by Owen (ref. 13). In this study the value of λ was assumed to be

$$\lambda = \frac{x_{cr}}{4} \tag{9}$$

which is consistent with the use of a Van Driest inner eddy viscosity law as suggested in reference 6. In this method, the sensitivity of changes in Re_{cr} to the predicted transition point was examined. Values of Re_{cr} = 2000, 3000, and 4000 have been used in conjunction with the velocity distributions corresponding to U_r = 58 and 149 meters per second (190 and 489 ft/sec) (see table II).

The boundary-layer program of reference 7 had provisions for including transition by specifying a factor analogous to $\Gamma(x)$ which determined what fraction of the effective viscosity was associated with turbulence. However, since $\Gamma(x)$ was an unknown in the present investigation, it was desirable to incorporate a semiempirical model of the transition process. This model, as applied to the present study, did not require the specification of a critical Reynolds number, but instead, the value of Re_{cr} was determined as a function of the pressure gradient parameter $\overline{K}$, given by

$$\bar{K} = \frac{\theta^2}{\nu_w} \frac{dU_\infty}{dx} \tag{10}$$

The function $Re_{cr}(\bar{K})$ was described empirically. After determining $Re_{cr}(\bar{K})$, the transition length was obtained from Granville's criterion (ref. 14), which also included the effects of free-stream turbulence intensity. The distribution of $\Gamma(x)$ in the transition region was based on the results of reference 12. Further details of the transition model can be obtained from reference 7. This model and the boundary-layer calculation method of reference 11 were used to predict transition on the plate at the lowest and highest velocity conditions (figs. 9(a) and (c), respectively). This method was used to determine the effect of free-stream turbulence intensity on the predicted transition location. The values of u'/U_∞ used in the analysis were 0, 0.01, and 0.04. As mentioned previously, the latter value of u'/U_∞ should represent the level of free-stream turbulence intensity associated with the flow in the vicinity of the plate model.

Comparison of Experimental and Predicted Transition

The experimental and predicted transition locations are listed in table III. Comparison of the results will also be made by superimposing the experimentally determined transition points from figure 9 on plots of the predicted distributions of $\Gamma(x)$. The results based on the method of reference 6 are presented in figures 11 and 12 for reference velocities U_r of 58 and 149 meters per second (190 and 489 ft/sec), respectively. The distributions are plotted for critical Reynolds numbers Re_{cr} of 2000 and 3000 in figure 11 and 2000, 3000, and 4000 in figure 12. (The distribution corresponding to Re_{cr} = 4000 is not shown in fig. 11 since predicted transition in this case did not occur within the length of the plate model.) At both the high- and low-reference-velocity conditions, a critical Reynolds number of 4000 yields a pronounced overprediction of the experimentally determined transition point. In order to optimize the predicted results for the two cases, it would be necessary to select a value of Re_{cr} between 2000 and 3000. In general, the calculations for $Re_{cr} = 3000$ resulted in a predicted transition point which exceeded the observed transition by as much as 40 percent. (The exception was the upper station low-velocity case, in which predictions indicated that transition occurred downstream of the plate model.) In general, the best predictions were obtained with the lowest value of Re_{cr} (2000) when combined with a transition length λ where $\lambda = x_{cr}/4$ (eq. (9)). Examination of table III indicates that for this case transition locations were underestimated from about 9 percent at the high velocity to about 30 percent at the low velocity.

It is also interesting to note that for $Re_{cr} = 2000$ the observed difference between the transition points at the upper and lower stations on the plate was predicted quite accurately. This can be noted in figures 11 and 12 by comparing the distance between the two experimental points with the distance between the predicted curves at $\Gamma = 1.0$.

The transition results based on the method of reference 7 indicated that, in general, the best predictions were obtained when the transition modeling was based on the 4-percent value of turbulence intensity. This appears to be consistent with the actual flow since turbulence intensities of about 4 percent were present near the leading edge (see fig. 5). Incorporation of this upper level of turbulence intensity ($u'/U_\infty = 0.04$) generally resulted in underestimations of X_t of about 20 to 50 percent, as shown in figures 13 and 14 and table III(b). Acceleration effects resulting from insertion of the plate possibly reduced the turbulence intensity level by 0.5 percent and thus extended the transition point farther downstream or in the direction of more favorable agreement.

DISCUSSION OF RESULTS

The results of this study indicated that the transition pattern on the plate was quite regular and well behaved. It is interesting to note that similar results were obtained in the compressor blade experiments of reference 1. Furthermore, as mentioned in reference 1, this result is in contrast to flat plate transition patterns, which are often jagged and irregular. Reference 1 attributes the irregularities in flat plate transition patterns to spanwise variations in free-stream turbulence. In the present study extreme care had to be maintained in applying the china-clay finish in order to obtain a regular smooth transition pattern, which suggests that surface roughness in the leading edge region was an important factor.

The limited results of this study tend to corroborate one of the conclusions of the compressor blade study of reference 1, that is, that a knowledge of the streamwise pressure gradient should be adequate to establish reasonable estimates of the transition location (in the absence of separation). Reference 1 suggests that the free-stream turbulence affects transition indirectly by varying the steamwise pressure distribution and causing changes in the rate of amplification of disturbances in the boundary layer.

The free-stream turbulence intensity did not enter explicitly in to the transition calculation method of reference 6. However, the effects on predicted transition location resulting from a variation in Re_{cr} were somewhat analogous to the effects resulting from a change in the free-stream turbulence intensity in the method of reference 7. Results from the analysis of reference 6 for a critical vorticity Reynolds number of 2000 were consistent with the results from the method of reference 7 for a free-stream turbulence intensity of 4 percent. As Re_{cr} was increased from 2000 to 4000, the predicted tran-

sition generally did not occur within the confines of the plate model. Similar results were apparent with the method of reference 7 when the free-stream turbulence intensity was reduced from 4 percent to zero.

In view of the uncertainties associated with the china-clay transition detection techniques as well as the relatively small scale of the test apparatus, the predicted results from both methods are considered reasonably good. It is apparent that in order to improve the predictions a better definition of the turbulence intensity in the flow field would be required. Also, the development of a relation between critical vorticity Reynolds number and free-stream turbulence intensity would be highly desirable, particularly since turbulence intensity appears to be a more measurable quantity than vorticity Reynolds number. The present study was conducted in a flow regime which provided a severe test of the prediction methods since turbulence levels were still in a range where small errors reflected large changes in the transition location (fig. 14).

SUMMARY OF RESULTS

The boundary-layer transition on a short plate was studied by means of the china-clay visual technique. The plate model was subjected to small simultaneous spanwise and chordwise pressure gradients. The studies were conducted at three nominal plate leading edge velocities ranging from 80 to 241 meters per second (263 to 789 ft/sec). Transition predictions were obtained from two finite-difference two-dimensional boundary-layer calculation methods which incorporated transition models based on the concept of a transition intermittency factor. Principal results of this study were as follows:

1. The transition patterns that were obtained were smooth rather than jagged and were similar to the patterns observed by others on compressor blades.

2. The transition patterns were appreciably curved in the spanwise direction. Translation of the curved transition pattern in the streamwise direction was attributable primarily to changes in Reynolds number.

3. Reasonable predictions of the observed transition location at two spanwise stations were obtained within the framework of recommended options in the boundary-layer calculation methods.

Lewis Research Center,
National Aeronautics and Space Administration,
Cleveland, Ohio, June 19, 1974,
501-24.

REFERENCES

1. Walker, G. J.: An Investigation of Boundary Layer Transition on an Axial-Flow Compressor Blade. ARL/ME-122, Aeronautical Research Labs., 1968.

2. Dunham, J.: Predictions of Boundary Layer Transition on Turbomachinery Blades. In AGARD Boundary Layer Effects in Turbomachines, Dec. 1972, pp. 55-71

3. Hall, D. J.; and Gibbings, J. C.: Influence of Stream Turbulence and Pressure Gradient Upon Boundary Layer Transition. J. Mech. Eng. Sci., vol. 14, no. 2, 1972, pp. 134-146.

4. McDonald, H.; and Fish, R. W.: Practical Calculations of Transitional Boundary Layers. Intern. J. Heat Mass Transf., vol. 16, no. 9, Sept. 1973, pp. 1729-1744.

5. Seyb, N. J.: The Role of Boundary Layers in Axial Flow Turbomachines and the Prediction of Their Effects. In AGARD Boundary Layer Effects in Turbomachines, Dec. 1972, pp. 241-259.

6. Miner, E. W.; Anderson, E. C.; and Lewis, Clark, H.: A Computer Program for Two-Dimensional and Axisymmetric Nonreacting Perfect Gas and Equilibrium Chemically Reacting Laminar, Transitional and/or Turbulent Boundary Layer Flows. VPI-E-71-8, Virginia Polytechnic Institute, May 1971.

7. Albers, James A.; and Gregg, John L.: Computer Program for Calculating Laminar, Transitional, and Turbulent Boundary Layers for Compressible Axisymmetric Flow. NASA TN D-7521, 1974.

8. Brinich, Paul F.; and Neumann, Harvey E.: Some Characteristics of Turbulent Boundary Layers in Rapidly Accelerated Flows. NASA TN D-6587, 1971.

9. Katsanis, Theodore; and McNally, William D.: Revised Fortran Program for Calculating Velocities on Streamlines on a Blade-to-Blade Stream Surface of a Turbomachine. NASA TM X-1764, 1969.

10. Batchelor, George K.: The Theory of Homogeneous Turbulence. Cambridge Univ. Press, 1953, p. 68.

11. Herring, H. J.; and Mellor, G. L.: Computer Program for Calculating Laminar and Turbulent Boundary Layer Development in Compressible Flow. NASA CR-2068, 1972.

12. Dhawan, S.; and Narashmha, R.: Some Properties of Boundary Layer Flow During Transition From Laminar to Turbulent Motion. J. Fluid Mech., vol. 3, pt. 4, Jan. 1958, pp. 418-436.

13. Owen, F. K.: Transition Experiments on a Flat Plate at Subsonic and Supersonic Speeds. AIAA J., vol. 8, no. 3, Mar. 1970, pp. 518-523.

14. Granville, Paul S.: The Calculation of the Viscous Drag of Bodies of Revolution. DTMB-849, David Taylor Model Basin, 1953.

TABLE I. - LOCATION OF TRANSITION ON PLATE MODEL AS DETERMINED FROM CHINA-CLAY METHOD.

[Plate length, 7.62 cm (3.0 in.).]

Reference velocity, U_r		Spanwise station (refer to fig. 2)	Transition location, $X_t = (x/L)_t$
m/sec	ft/sec		
58	190	Upper	0.99
		Lower	.89
87	285	Upper	0.73
		Lower	.66
149	489	Upper	0.50
		Lower	.44

TABLE II. - EDGE VELOCITIES ON PLATE MODEL BASED ON MEASURED WALL PRESSURES

[Plate length, 7.62 cm (3.0 in.).]

Distance from leading edge, X = x/L	Upper station (refer to fig. 2)						Lower station (refer to fig. 2)					
	Reference velocity, U_r											
	58 m/sec	190 ft/sec	87 m/sec	285 ft/sec	149 m/sec	489 ft/sec	58 m/sec	190 ft/sec	87 m/sec	285 ft/sec	149 m/sec	489 ft/sec
	Edge velocity, U_e											
	m/sec	ft/sec	m/sec	ft/sec	m/sec	ft/sec	m/sec	ft/sec	m/sec	ft/sec	m/sec	ft/sec
[a]0	72.8	239	111.3	365	218.5	717	80.2	263	122.2	401	240.5	789
.10	76.2	261	119.2	391	244.1	801	86.3	283	130.8	429	269.7	885
.23	85.3	280	129.8	426	264.9	869	88.7	291	133.5	438	274.3	900
.40	83.2	273	126.2	414	254.8	836	85.3	280	129.8	426	259.4	851
.57	81.1	266	123.7	406	249.0	817	83.2	273	126.2	414	249.3	818
.73	80.5	264	123.1	404	248.1	814	81.7	268	124.1	407	246.3	808
.90	81.1	266	123.7	406	250.5	822	82.0	269	124.4	408	249.0	817

[a]Leading edge velocities determined by interpolation procedure.

TABLE III. - COMPARISON OF EXPERIMENTAL AND PREDICTED TRANSITION ON PLATE MODEL

[Plate length, 7.62 cm (3.0 in.).]

(a) Theoretical results based on method of reference 6

Experiment				Theory		
Reference velocity, U_r		Spanwise station (refer to fig. 2)	Transition location, $X_t = (x/L)_t$	Critical Reynolds number, Re_{cr}		
m/sec	ft/sec			2000	3000	4000
				Transition location, $X_t = (x/L)_t$		
58	190	Upper	0.99	0.72	(a)	(a)
		Lower	.89	.63	1.00	(a)
149	489	Upper	0.50	0.46	0.70	0.83
		Lower	.44	.40	.53	.66

[a]Predicted transition did not occur on plate model.

(b) Theoretical results based on method of reference 7

Experiment				Theory		
Reference velocity, U_r		Spanwise station (refer to fig. 2)	Transition location, $X_t = (x/L)_t$	Free-stream turbulence intensity, u'/U_∞		
m/sec	ft/sec			0	0.01	0.04
				Transition location, $X_t = (x/L)_t$		
58	190	Upper	0.99	(a)	(a)	0.53
		Lower	.89	(a)	(a)	.50
149	489	Upper	0.50	(a)	(a)	0.40
		Lower	.44	0.38	0.30	.21

[a]Predicted transition did not occur on plate model.

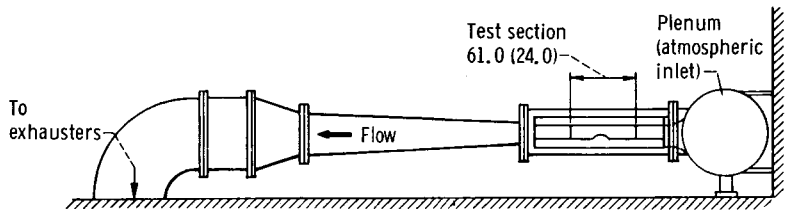

(a) Wind tunnel.

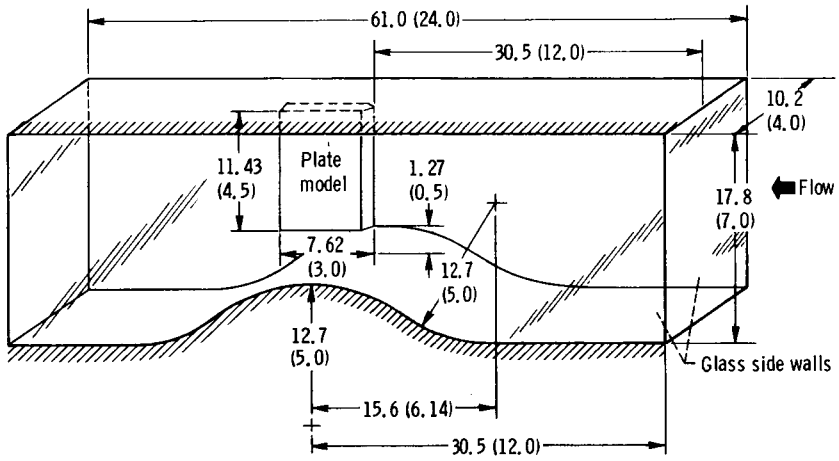

(b) Test section.

Figure 1. - Test facility. (Dimensions in centimeters (in.).)

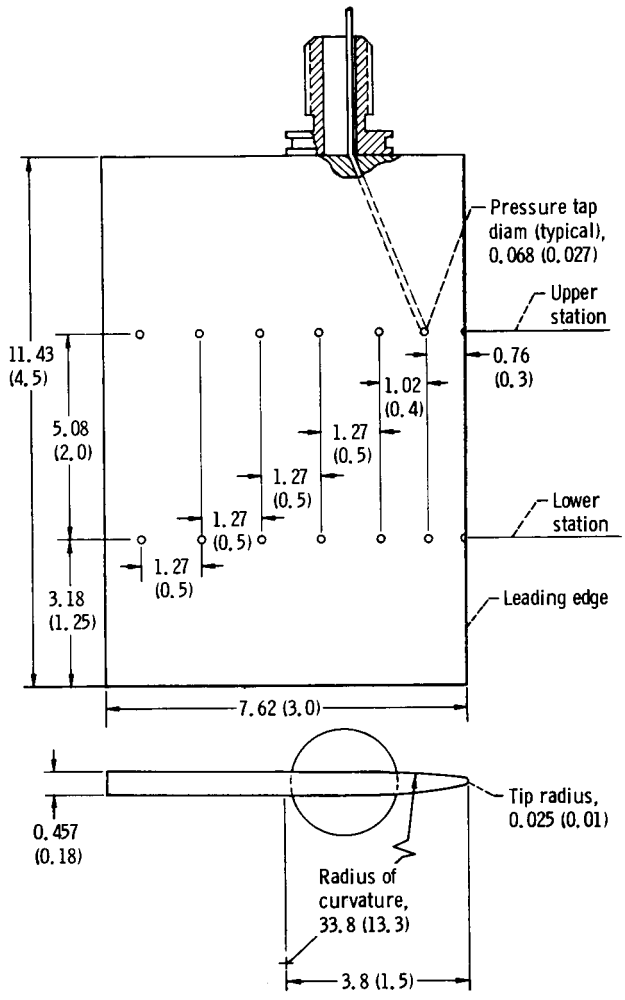

Figure 2. - Diagram of plate model and instrumentation.
(Dimensions in centimeters (in.).)

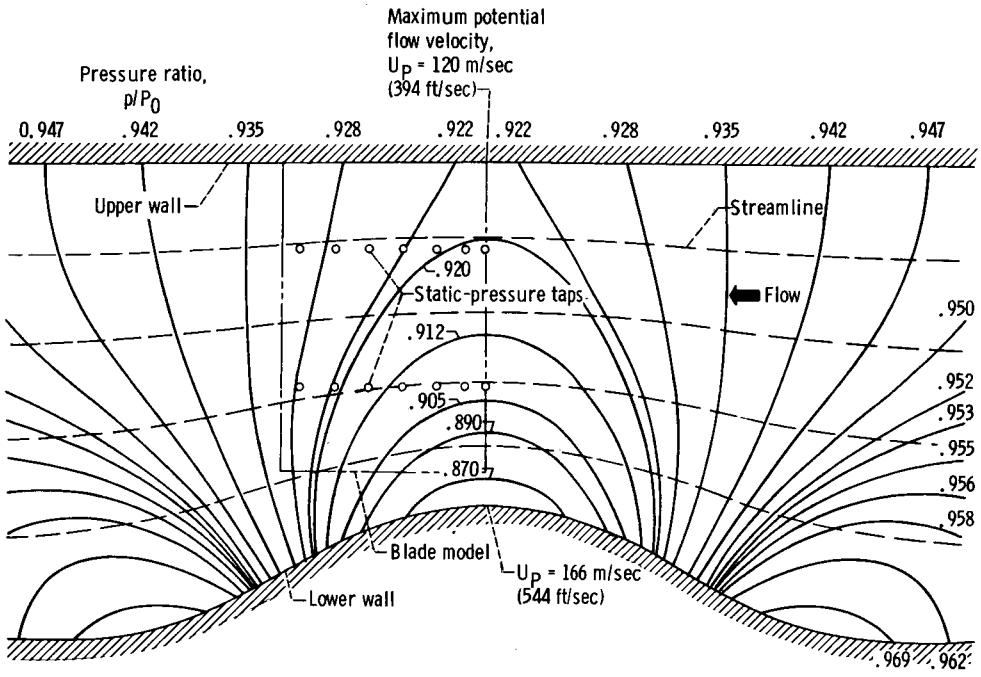

Figure 3. - Potential flow field in test section calculated by using method of reference 9. Reference velocity, 91 meters per second (300 ft/sec).

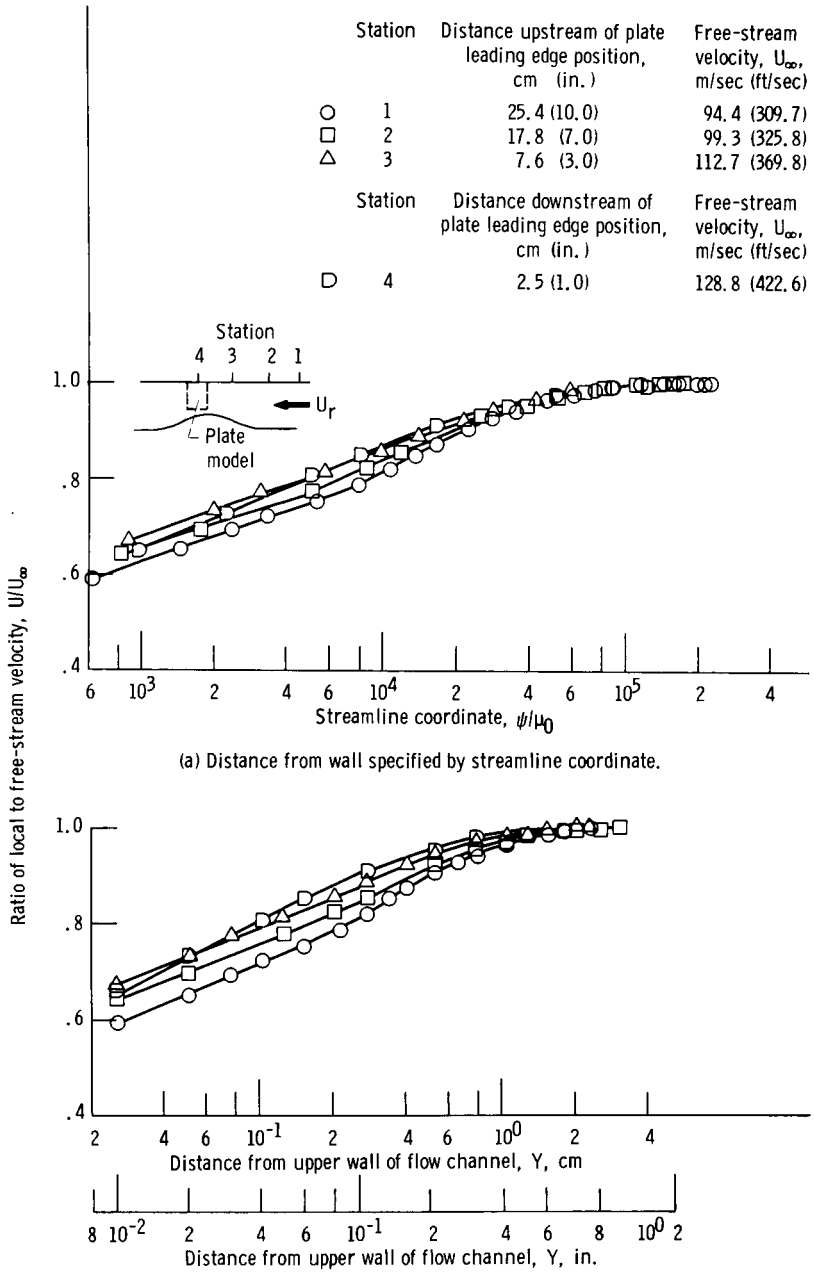

(a) Distance from wall specified by streamline coordinate.

(b) Distance from wall specified by dimensional coordinate.

Figure 4. - Distribution of velocity at four stations along upper wall of flow channel with plate removed. Reference velocity, 94.4 meters per second (309.7 ft/sec).

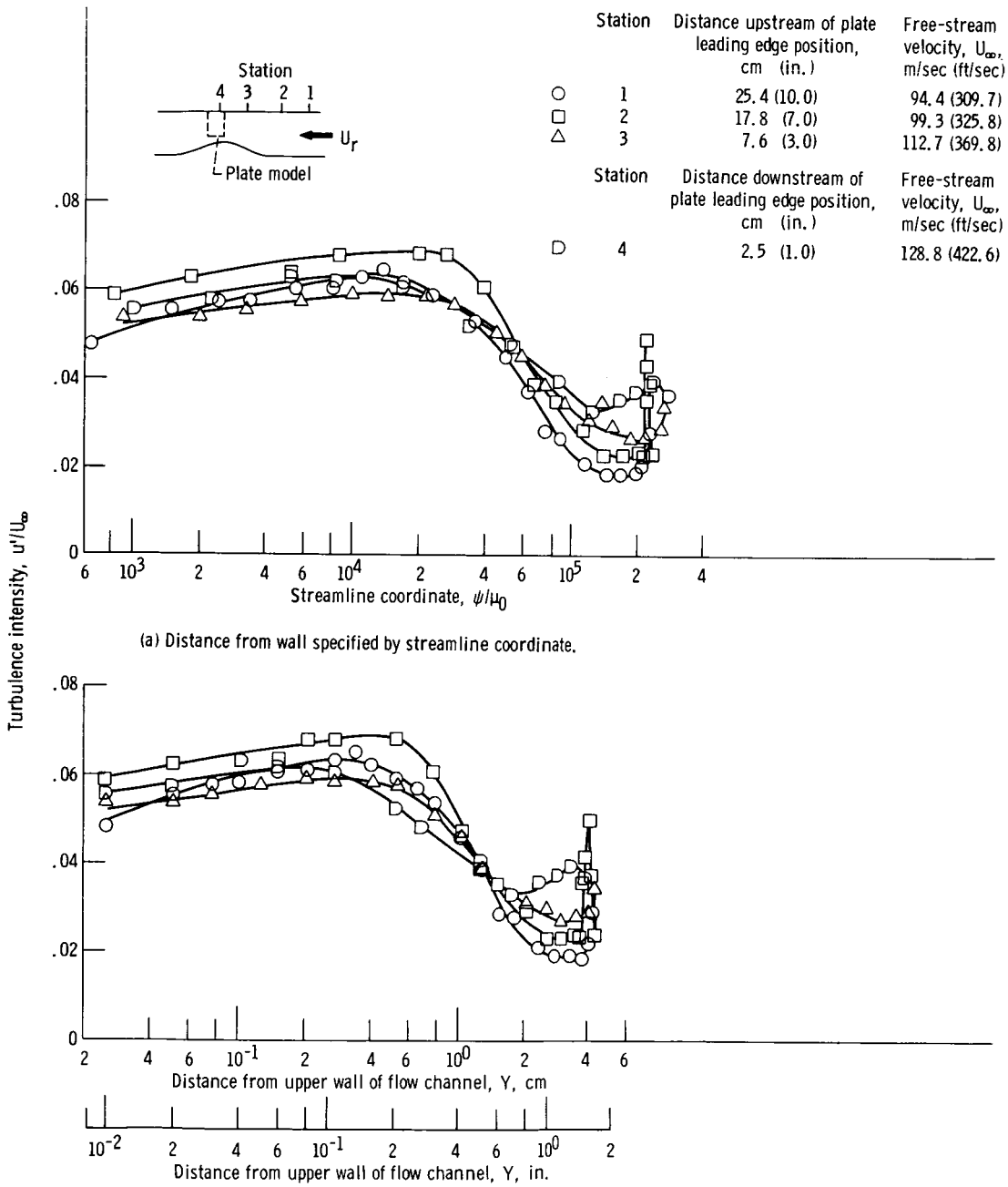

(a) Distance from wall specified by streamline coordinate.

(b) Distance from wall specified by dimensional coordinate.

Figure 5. - Distribution of turbulence intensity at four stations along upper wall of flow channel with plate removed. Reference velocity, 94.4 meters per second (309.7 ft/sec).

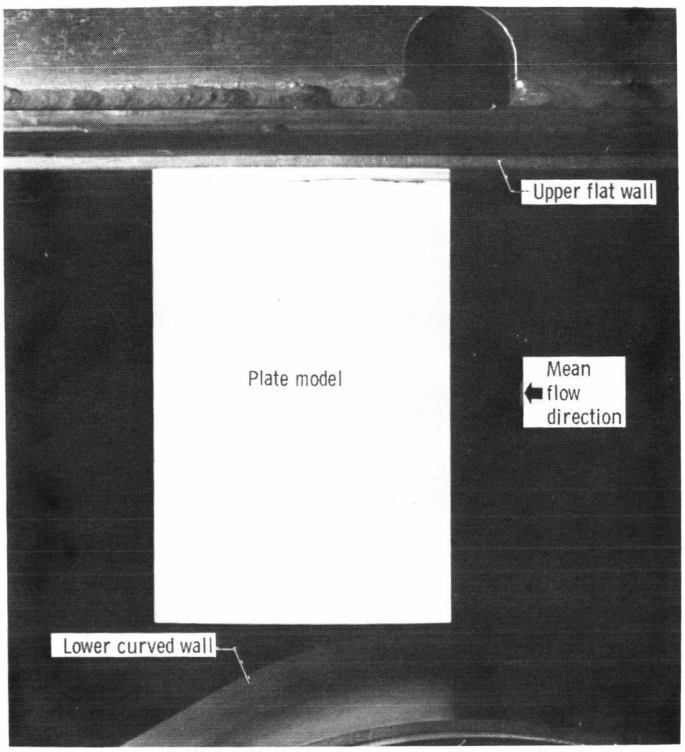

Figure 6. - Plate model after spraying with china-clay solution.

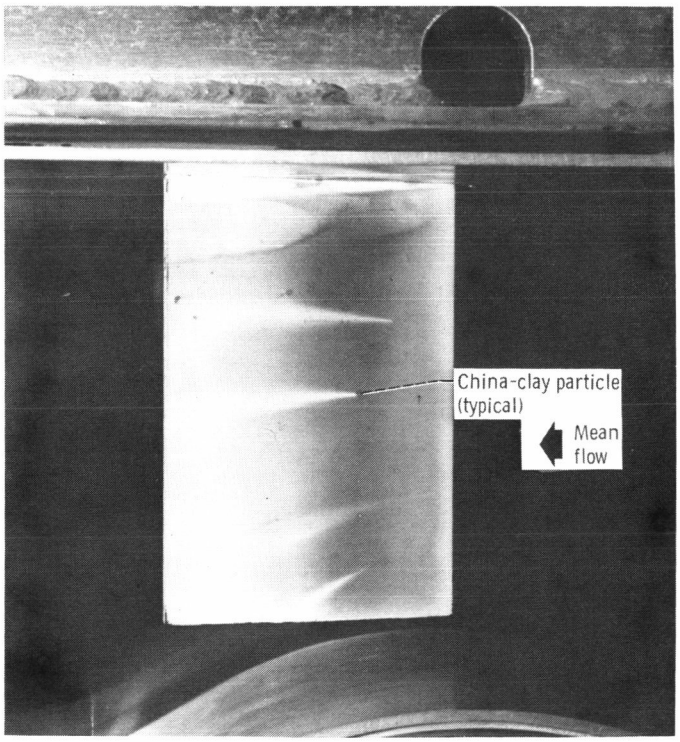

Figure 7. - View of plate model showing effects of random surface protuberances on transition pattern.

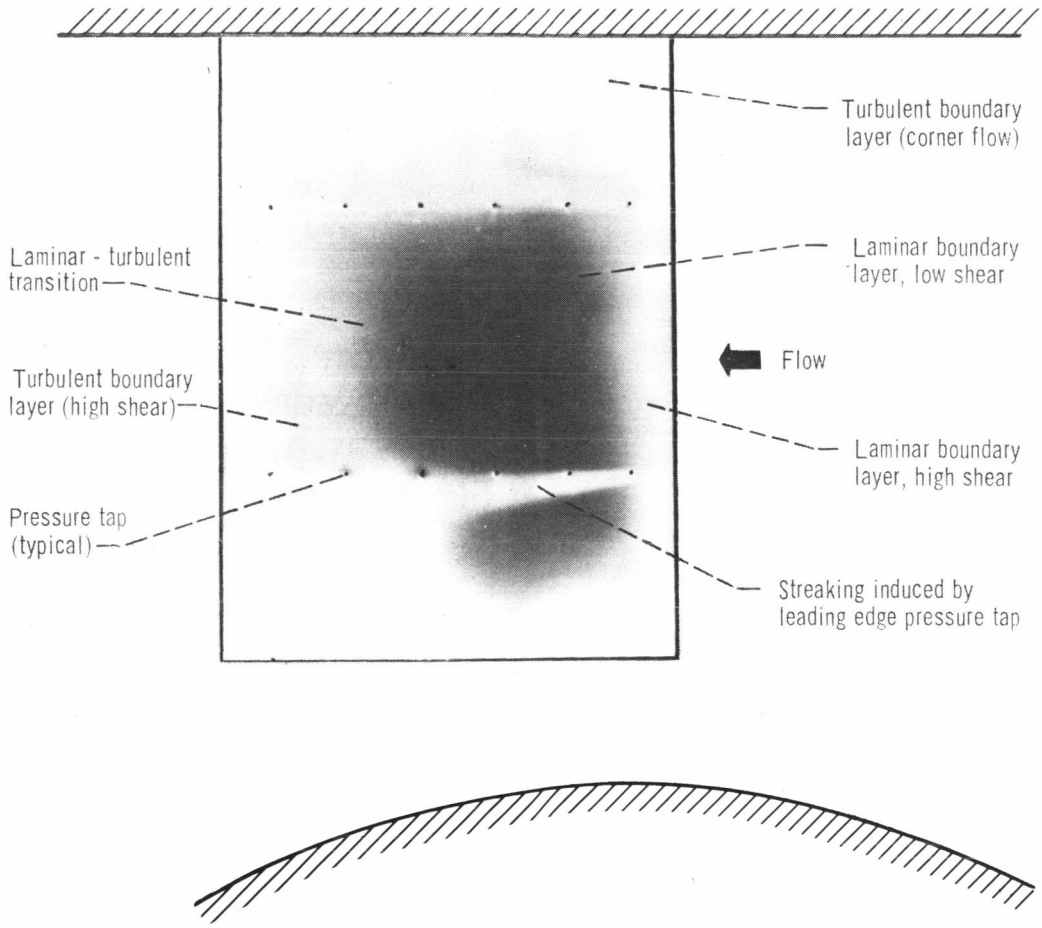

Figure 8. - Interpretation of photographs of transition using china-clay visual method.

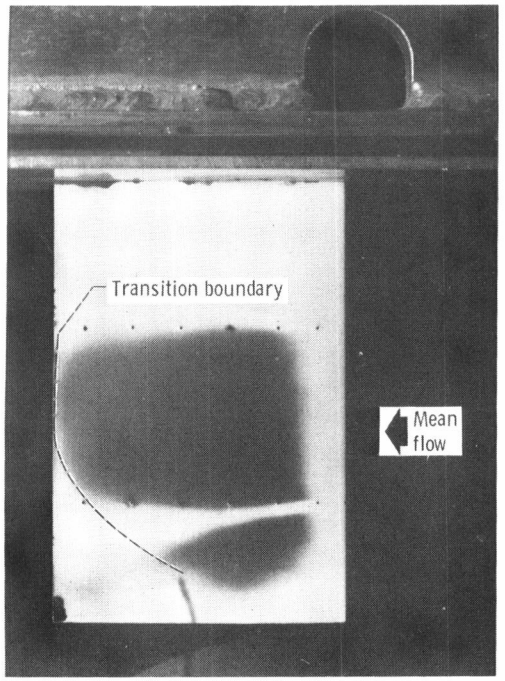

(a) Reference velocity, 58 meters per second (190 ft/sec).

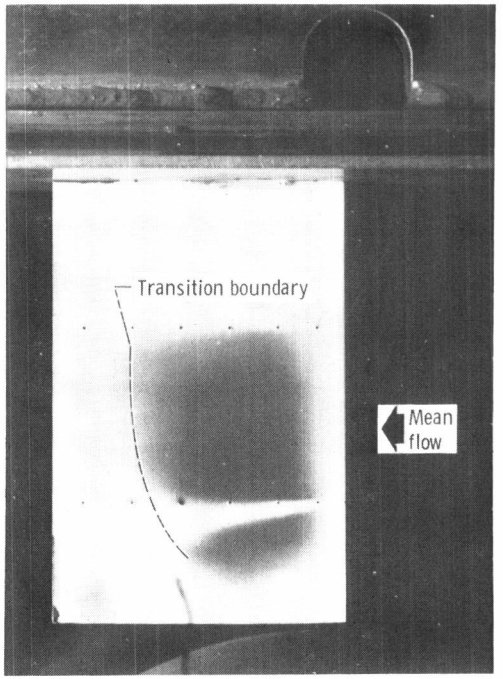

(b) Reference velocity, 87 meters per second (285 ft/sec).

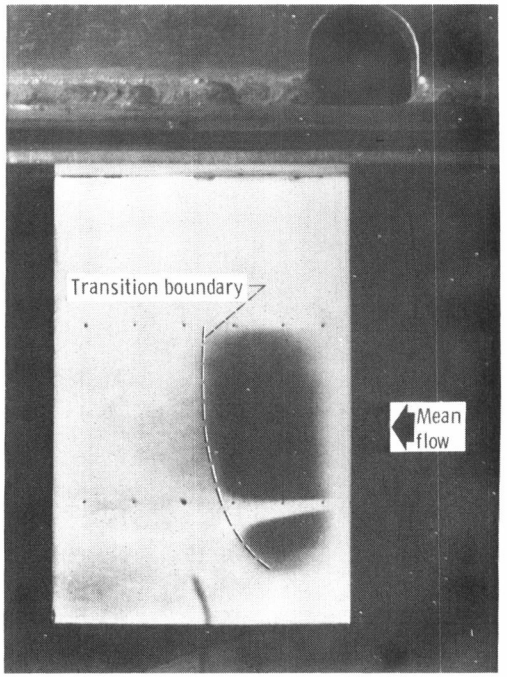

(c) Reference velocity, 149 meters per second (439 ft/sec).

Figure 9. - Transition on plate for various upstream velocities.

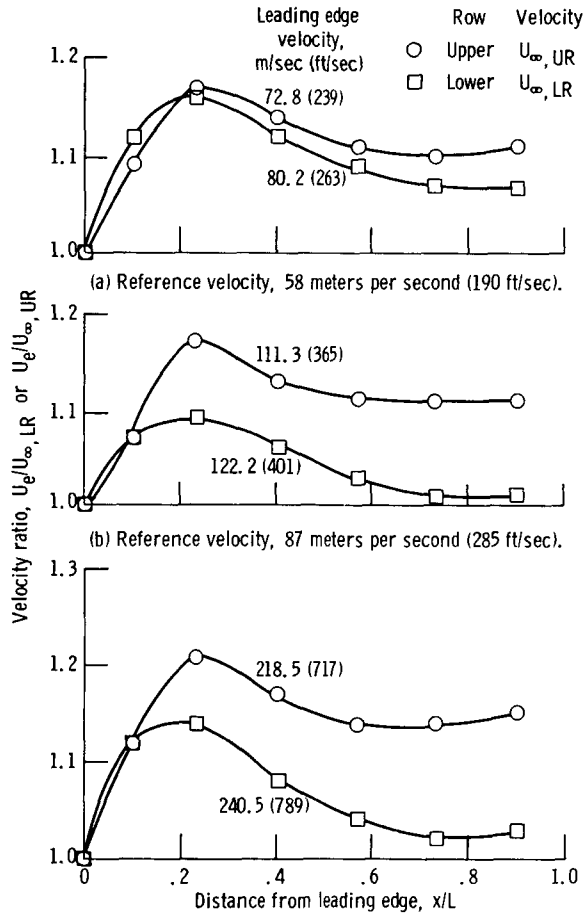

(a) Reference velocity, 58 meters per second (190 ft/sec).

(b) Reference velocity, 87 meters per second (285 ft/sec).

(c) Reference velocity, 149 meters per second (489 ft/sec).

Figure 10. - Edge velocity distributions on plate model. Plate length, 7.62 centimeters (3.0 in.).

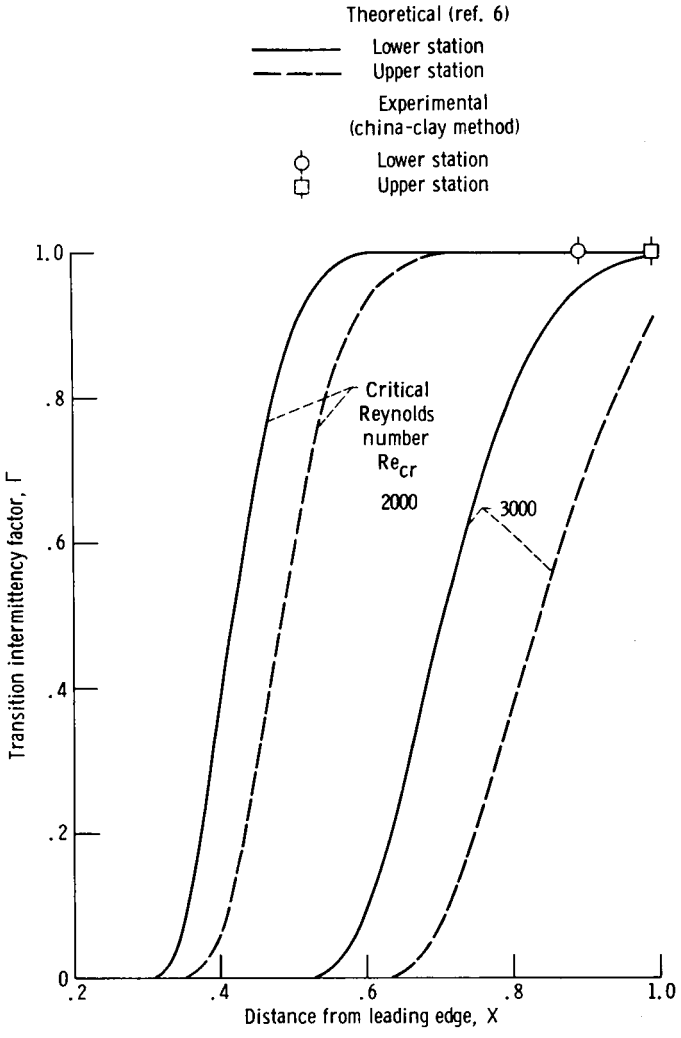

Figure 11. - Distributions of predicted transition intermittency factor based on method of reference 6. Reference velocity, 58 meters per second (190 ft/sec).

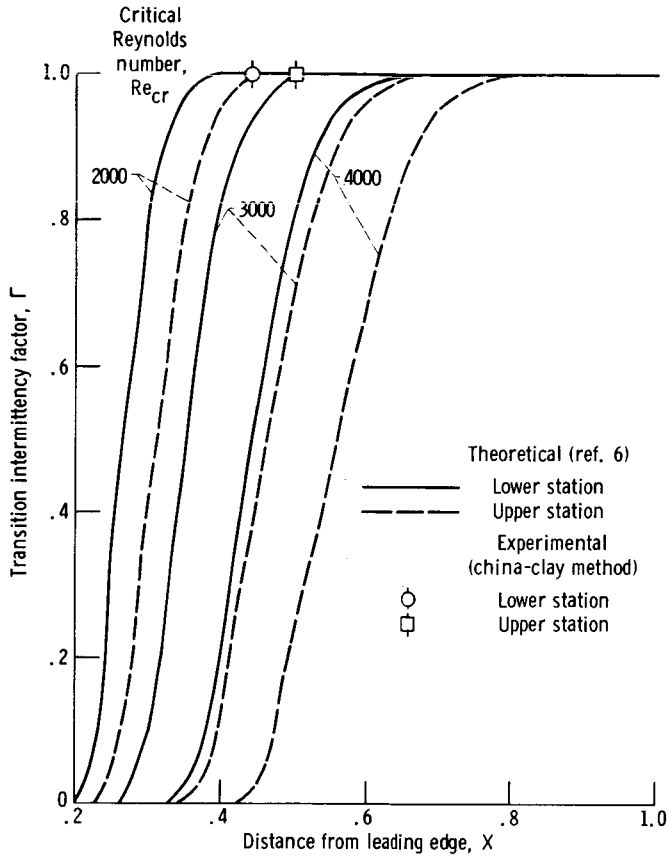

Figure 12. - Distributions of predicted transition intermittency factor based on method of reference 6. Reference velocity, 149 meters per second (489 ft/sec).

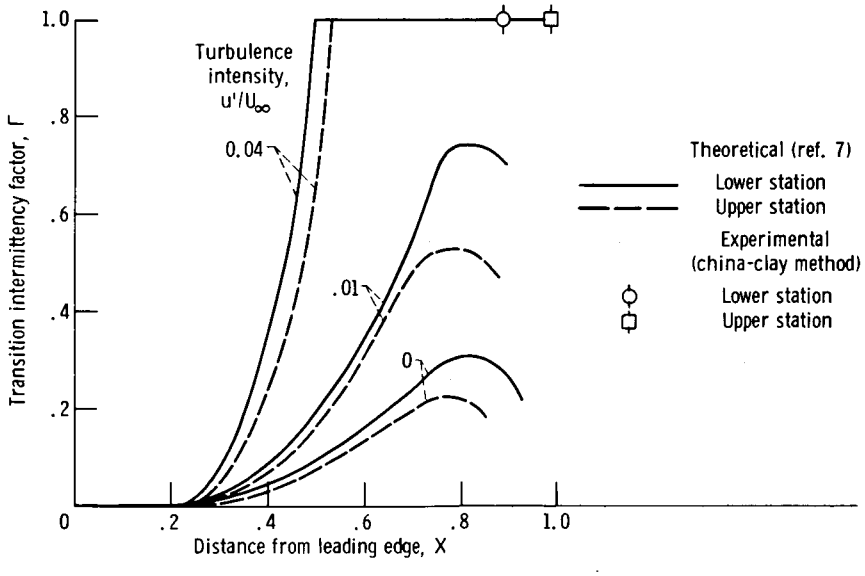

Figure 13. - Distributions of predicted transition intermittency factor based on method of reference 7. Reference velocity, 58 meters per second (190 ft/sec).

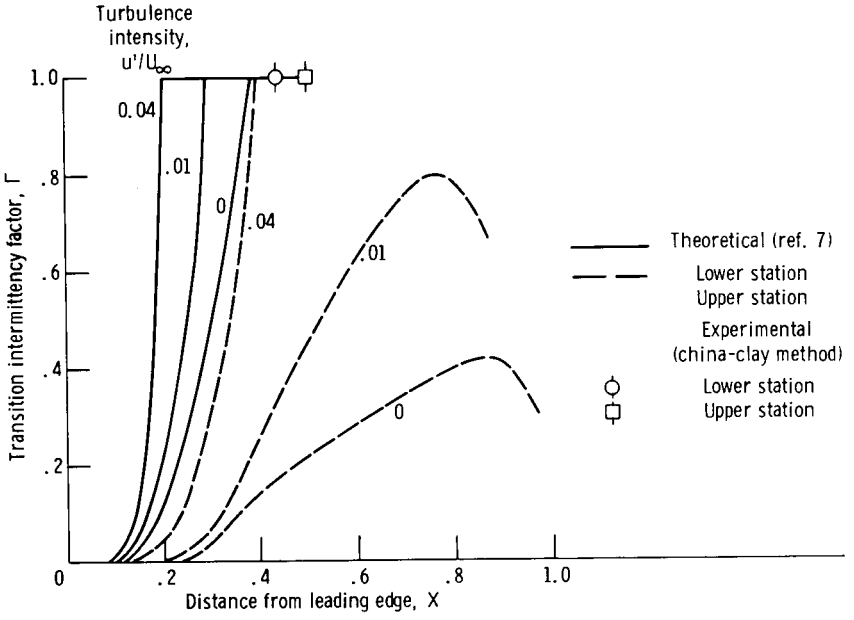

Figure 14. - Distributions of predicted transition intermittency factor based on method of reference 7. Reference velocity, 149 meters per second (489 ft/sec).

NASA-Langley, 1974 E-7979